Atmospheric Pollution Research 6 (2015) 612-617

Short Communication

Atmospheric Pollution Research

www.atmospolres.com

Effect of air velocity on nanoparticles dispersion in the wake of a vehicle model: Wind tunnel experiments

Amine Mehel [1], Frederic Murzyn [2]

[1] *ESTACA'Lab, Transportation Mechanics Laboratory, ESTACA, 92300, Levallois, France*
[2] *ESTACA'Lab, Transportation Mechanics Laboratory, ESTACA, 53061, Laval, France*

ABSTRACT

Exposure to nanoparticles coming from road–traffic concerns a large part of urban population in both outdoor and indoor environments leading to the enhancement of short and long–term health problems. The dynamics of such small particles is very sensitive to the turbulent diffusion and Brownian motion. Hence their concentrations are dependent on the flow structure properties (length and time scales). In this paper, a wind tunnel study is conducted to assess the effect of the flow on the dispersion of nanoparticles coming out from tailpipe in the near–wake of a reduced–scale truck model. Particle number concentration (PNC) measurements are achieved at 66 positions downstream of the model. Our results point out that the interaction of the ultrafine particles (UFP) with the vortices appearing in the near–wake of a truck enhances their dispersion in both transversal and vertical directions. Increasing the inflow air velocity strengthens this spreading. Overall, we demonstrate that such wind tunnel measurements are fundamental to improve our knowledge on the existing interaction between road–traffic, turbulence and particle concentration to accurately evaluate human exposure rates to ultrafine particles and their potential consequences.

Keywords: *Vehicle emissions, aerodynamics, ultrafine particle dispersion, wind tunnel, turbulence*

Corresponding Author:
Amine Mehel
☎ : *+33-1-41276024*
🖷 : *+33-1-41273742*
✉ : *amine.mehel@estaca.fr*

Article History:
Received: 10 April 2014
Revised: 14 January 2015
Accepted: 14 January 2015

doi: 10.5094/APR.2015.069

1. Introduction

Particles involved in air pollution are a mixture of ultrafine, fine and coarse particles. They mainly consist of combustive byproducts as well as biological materials. In urban areas, engine combustion emissions associated with the road traffic are one of the major sources of fine and ultrafine particles number concentrations (PNC) in which ultrafine particles (UFP) are the dominant contributor. They roughly account for 90% or more of the total particle number in areas influenced by on–road vehicles emissions (Morawska et al., 2008). Indeed, recent studies have reported high concentrations of ultrafine particles (diameter below 100 nm) in the vicinity of roadways (Zhu et al., 2002; Kittelson et al., 2004; Hudda et al., 2012). As a consequence, adjacent indoor environments in urban areas, such as buildings or offices, may experience significant concentrations of outdoor ultrafine particles due to their infiltration, exposing occupants to potentially toxic pollutants (Zhu et al., 2005). Several health effects are associated with nanoparticles exposure. Indeed, many toxicological and epidemiological studies have associated the exposure to UFP to the enhancement of allergy, inflammation and asthma (Diaz–Sanchez et al., 2003) and cardiac disease (Verrier et al., 2002; Delfino et al., 2005). It is relevant to note that UFP can penetrate into cell membranes, blood and reach the brain (Oberdorster et al., 2004). Pope et al. (2002) concluded from mortality data over 500 000 individuals that for every increase of 10 µg/m^3 in fine particles (particles with a diameter below 2.5 µm), the risk of all–cause, cardiopulmonary and lung cancer mortality increased by 4%, 6% and 8%, respectively.

Dealing with the infiltration, several studies have reported that penetration of particles from outdoor origin into indoor environments is significant and depends on exchange rates, dimensions of building cracks and on physico–chemical characteristics of particles. Through cracks, Liu and Nazaroff (2003) and Jeng et al. (2007) showed that particle penetration is almost complete for particles with diameters below 7 µm with cracks of 1 mm or higher, and for particles ranging from 0.1–1 µm for cracks size below 0.25 mm. For the other cases, particle deposition depends on cracks roughness and shapes. Furthermore, the results confirm that particle infiltration in the buildings is a complex problem. It does not only depend on crack properties but also on particle characteristics. These same characteristics also influence their dispersion until they reach the building envelope cracks. Indeed, because of their small size and low Stokes number, the dynamics of these nanoparticles is not only influenced by turbulent dispersion and Brownian diffusion but also by thermophoresis or electrophoresis when external fields are present (temperature gradients or electric potential difference, respectively). The effect of these different mechanisms depends on the particle size (Mehel et al., 2012). To date, little is known about the interaction between nanoparticles exhausting from tailpipes and vehicle wakes and on the way on how it could influence their spatial and temporal evolutions and thus their movements towards the surrounding environment. Among the few studies available on this topic, Carpentieri and Kumar (2011) used an on–board grid measurements mounted at the rear of a vehicle in the near–wake region with a total of 9 sensors located at different heights and transversal positions and at distances of 0.45 m and 0.8 m from the rear

bumper. Their measurements gave an idea on particle dispersion but are limited since the investigated area only concerns a region located at a short distance from the vehicle. In the last 10 years, some studies were conducted in wind tunnels (Kanda et al., 2006; Carpentieri et al., 2012). The near–wake region was investigated and more accurate data have been recorded leading to improved results. It was clearly shown that the vehicle wake influences the dispersion of the pollutants. Nevertheless, only gaseous pollutants were concerned which do not necessarily reflect the UFP dynamics because soot nanoparticles undergo fast transformation processes after being released from the tailpipe (Carpentieri and Kumar, 2011) while the passive tracer gas is only affected by dilution. It is worthwhile to note that soot particles are primarily composed of carbon and their size changes during the dilution process by condensation of gaseous molecules on particle surfaces. As a consequence the particle size is rapidly changing due to these deposition and decomposition mechanisms, thus influencing their movement. Indeed the Brownian motion, the turbulent diffusion or the turbophoresis depend on the relative inertia of the particles in the range of 10 nm–5 µm (Mehel et al., 2010).

In the present paper, wind tunnel experiments are conducted to study the dynamics of carbonaceous UFP downstream of a reduced–scale truck model. PNC measurements are achieved to bring new understanding regarding UFP interaction with the flow structure in the near–wake region of a vehicle and its consequences on their dispersion. The results lead to a more comprehensive and accurate picture on UFP distribution/accumulation downstream of a vehicle. Potential applications of such investigations include, but are not limited to, correlation between outer and in–cabin concentrations. After this introduction, the experimental method and the instrumentation are described in Section 2 followed by the presentation of the results. The discussion is developed in Section 3. Finally some conclusions and possible future works are suggested in Section 4.

2. Experimental Method and Instrumentation

The PNC measurements were conducted in the experimental facility at ESTACA Paris. The wind tunnel has a test section which is 800 mm in length, 600 mm in width and 600 mm in height. An unfiltered air at approximately 300 K and 45 to 70% of relative humidity was used with an inflow velocity ranging from 0 to 25 m/s. Two inflow air velocities are investigated in the present study ($U_{m\infty}$=14.25 m/s and 23.75 m/s). The incoming flow is supposed to undisturbed with a low level of turbulence (less than 1%). We aim at investigating the dispersion of exhausted UFP in urban areas downstream of a reduced–scale truck model. The experimental conditions correspond to real truck prototype speeds of $U_{p\infty}$=8.33 m/s (30 km/h) and $U_{p\infty}$=13.88 m/s (50 km/h) respectively, also corresponding to two typical urban speeds. The associated Reynolds number, based on the truck prototype height h_p and kinematic viscosity of air ($Re_p=U_{p\infty}\ h_p/\nu$), is larger than $9.56\text{x}10^6$, while the Reynolds number of the reduced–scale truck model is larger than $6.2\text{x}10^6$. This is significantly above the critical value of 10^4 from which the boundary layer at the rear of the vehicle becomes turbulent. Above this limit, little sensitivity to the Reynolds number is expected according to Hucho (1998). Thus, we acknowledge that the dynamic similarity is ensured for both speeds.

The kinematic scale factor defined as $U_{m\infty}/U_{p\infty}$ is set to 1.71 to enhance the signal to noise ratio in terms of PNC. The same factor must be applied to the exhaust gas/particles velocity given the engine speed of 2 500 rpm. This implies an exhaust velocity at the truck prototype tailpipe (for a four stroke cycle engine) written as:

$$U_{pj} = \frac{V_{cyl}}{30\,000}\,\frac{\Omega}{\pi D_{pj}^2}\,\eta \tag{1}$$

where V_{cyl} is the cylinder swept volume in L, Ω is the engine speed in rpm, D_{pj} is the prototype tailpipe diameter in m and η is the volumetric efficiency.

The studied vehicle model represents the common rear part of trucks with a size reduced by a scale factor of 1/20 compared to the real prototype size (Figure 1). The emission point representing the model exhaust pipe is located at the bottom left quarter of the model as on most of vehicles.

The coordinate system is sketched on Figure 1. The *x* axis corresponds to the main flow stream, the *y* axis being the transversal direction and z the vertical axis, positive upward. The origin (0, 0, 0) is located at the rear of the vehicle model with *x*=0 m, *y*=0 m at the centerline, and *z*=0 m at ground level. For data analysis, dimensionless distances (*X*, *Y*, *Z*) are used which are given by *X*=*x*/*h*, *Y*=*y*/*h*, and *Z*=*z*/*h*, where *h*=0.065 m is the model height. In this non–dimensional coordinate system, the injection point representing the tailpipe is located at (0, –0.25, 0.25).

The generation of the UFP is ensured through the use of the PALAS DNP 2000 spark discharge aerosol generator using graphite electrodes and Nitrogen. The generated carbonaceous particle sizes range from 20 nm to 100 nm. They are found to be analogous to combustion aerosols in structure, particularly to diesel soot (Evans et al., 2003). The aerosol is injected in the model tailpipe at a flow rate of *Q*=0.133 L/s. An Electrical Low Pressure Impactor (ELPI) is used for particle number concentration measurements. The sampling grid is composed of a total of 66 points in the longitudinal, transversal and vertical directions at positions ranging between $0.5<X<5$, $-1<Y<1$ and $0.25<Z<0.75$. For each position, data acquisition lasts about 120 s. This was necessary to ensure the accuracy of the time–averaged particle concentrations. Furthermore, this is supposed to be large enough compared to the time scales of the flow.

For all measurements, we also consider a constant air speed (steady conditions) and no heat flux from engines. It should be noticed that even if the aerosol is not heated, the particles are less sensitive to the buoyancy than if a gaseous passive tracer were used.

3. Results and Discussion

First, the distribution of the time–averaged particle size (PSD) measured near the emission point (*X*=0.5, *Y*=0, *Z*=0.25) is presented in Figure 2. It shows that most of the particles concerned by PNC measurements have a size below 150 nm with prevalence for particles with a mean geometric diameter of about 40 nm. This is associated with a PNC of roughly 10^7 particles/cm^3. These results are consistent with those obtained from experimental investigations by Uhrner et al. (2007) with on–board measurements for a diesel engine and at the same engine speed, i.e. 2 500 rpm.

It is worthwhile to note that this PSD is averaged over a period of 120 s representing the duration of a single measurement as described above. It can be observed that even if the distance between the emission and the sampling points is quite short and since the PNC levels of the generated nanoparticles are greater than 10^6 particles/cm^3, it is large enough to observe that the emitted nanoparticles undergo fast transformation as reported by Carpentieri and Kumar (2011). In particular, they agglomerate to form relatively larger particles. This explains why the PNC of particles with size greater than 100 nm is not equal to the atmospheric level (about 10^3 particles/cm^3) but reaches nearly $0.8\text{x}10^5$ particles/cm^3 and $2.2\text{x}10^5$ particles/cm^3 for particles with mean geometric diameters of 137 nm and 215 nm, respectively. On the other hand, from the experimental results we only notice a slight change of the mean PSD with the transversal, longitudinal and vertical sampling positions even if the maximum levels of the concentrations decrease with the increase of the distance to the emission point. This tends to prove that particles rapidly agglomerate close to the exhaust pipe.

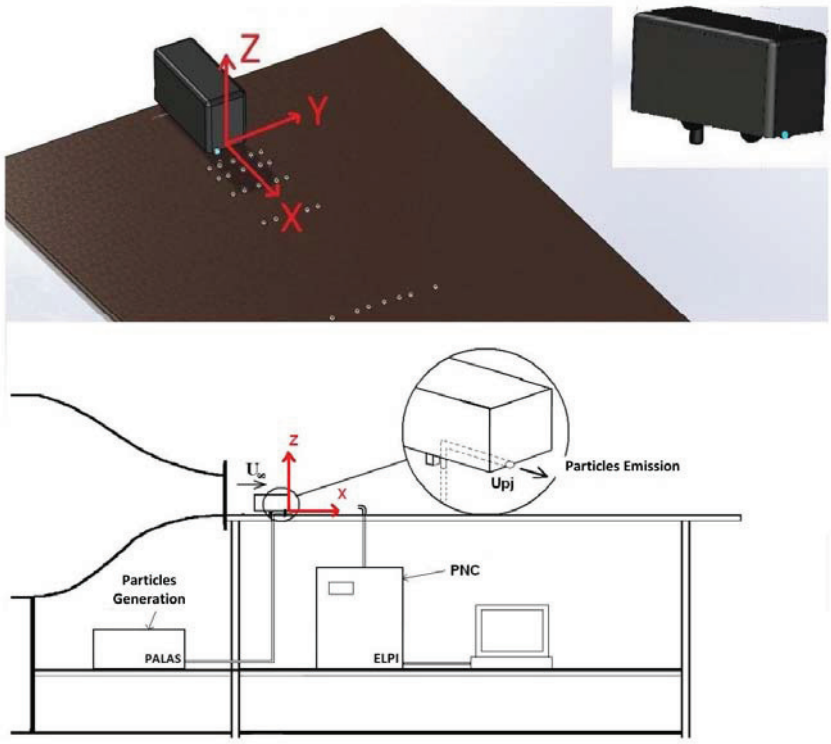

Figure 1. *Schematic of the experimental setup and the wind tunnel floor with the locations of the PNC measurement points.*

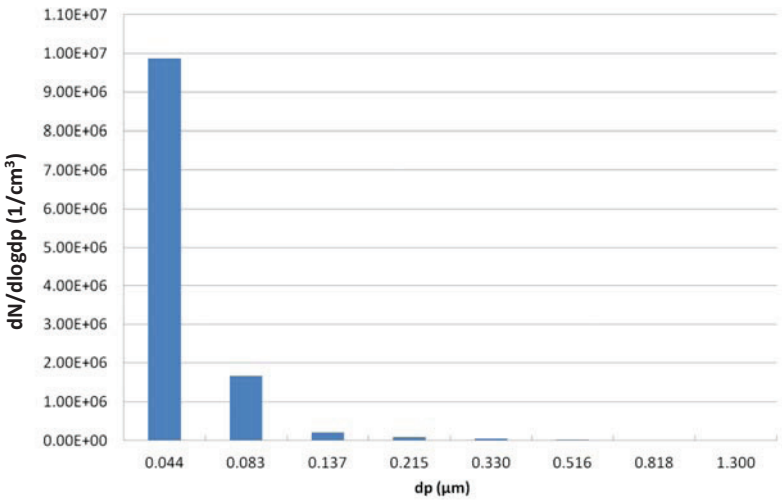

Figure 2. *Particle size distribution of the nanoparticles at (X, Y, Z)=(0.5, 0, 0.25).*

In the following part, the concentrations results are presented in terms of time–averaged PNC normalized by the maximum concentration obtained respectively for each wind–tunnel airflow velocity studied.

Figure 3a and 3b show a comparison of the horizontal profiles of nanoparticles dispersion for two typical urban speeds, i.e. 30 km/h and 50 km/h in the near wake region at *X*=0.5. We can notice that the peak of concentration corresponds to the vehicle centerline and not the emission plane centerline as in Carpentieri et al. (2012), but as confirmed by this latter study, the results are very sensitive to the probe/emission point positioning. This makes it difficult the comparison between different studies since also the vehicle shape has its own influence. Indeed, the vehicle near wake

is composed of two distinct regions: the first one very close to the vehicle (X<0.5), in the centerline, where it is dominated by a large recirculation vortice; the second one, at the vehicle lateral outer edges where longitudinal vortices develop (Hucho, 1998). The size of these two regions depends on the vehicle shape and velocity. This induces an emission point that could be found in both the recirculation vortices or in the outer longitudinal ones. When comparing Figure 3a and 3b corresponding to the transversal concentration profiles (normalized by the maximum concentration) at X=0.5 and for two vertical positions Z=0.25 and 0.75 respectively, we can see that a particle concentration peak is present at the vehicle center and for both dimensionless heights. This means that when particles are emitted they are sucked by the central recirculation region that diffuses them in the vertical direction. Farther from the vehicle but still in the near wake region (for 2<X<5), Figure 3c and 3d, show that the concentration profiles are flatter depicting a particle dispersion that is achieved more in the horizontal direction than in the vertical one as it was the case at X=0.5. In this region, the longitudinal vortices that developed at the outer edges of the vehicle are the only coherent structures. Thus, they are the main means for nanoparticles to be trapped and mixed.

On the other hand, the increase in the vehicle speed expand the particle dispersion in the transversal direction in the very near wake region (X<0.5) and in the lateral outer edges wake region (1<X<5). This is the result of an increasing vorticity.

Furthermore, from Figure 3a, a transversal dissymmetry is depicted around Y=0 for the higher speed. Indeed, in the very near wake region corresponding to 0.5<X<2, the concentration profile for the vehicle speed of 30 km/h is centered and that the particle dispersion is mostly achieved in the vertical direction (Figure 3a) whereas at 50 km/h it is seen that the exhaust plume is stretched on the left side (exhaust pipe location). As a consequence, the particles dispersion is achieved horizontally and vertically. When comparing the profiles at $U_{p\infty}$=30 and 50 km/h, we can conclude that the bias toward negative Y prevails through the plume height. At X=5, Z=0.25, we can notice the presence of a double peak that is more intense for $U_{p\infty}$=50 km/h, (Figure 3c) this could be correlated to the flow modification. It is believed that the intensity and dimension of the pair of the longitudinal vortices have increased. As a general trend for Figure 3, it can be observed that the measured plume is far from the classical Gaussian form, especially in the near wake region, for a vehicle speed higher than 50 km/h. Nevertheless, this assumption is often taken into account to build mathematical models. This finding has also been reported by Kanda et al. (2006) and Carpentieri et al. (2012). The nanoparticles being very sensitive to the turbulent structures, their mixing and dispersion are a more complex phenomenon than a simple Gaussian diffusion. However, for the transversal dispersion described by Carpentieri et al. (2012), the gaseous pollutants seem to be driven to the centerline as in the present study using solid nanoparticles. This is not similar to the study of Kanda et al. (2006) where the concentration peak is in line with the transversal plane of the exhaust pipe for the truck model.

Figure 4 clearly highlights the influence of the vortices in particle dispersion. Figure 4a shows the concentration profiles in the vehicle centerline plane (Y=0) and at a height of Z=0.25, it can be noticed that the concentration is the highest in the very near wake region corresponding to 0.5<X<2 and decreases sharply for X>2. The same trend is observed at both speeds 30 km/h and 50 km/h. When looking at the same profiles in the plane Y=–0.3 at Z=0.25 (Figure 4b), we can notice that the concentration is 5 times lower than the one in the centerline at X=0.5 and 3 times at X=1 for $U_{p\infty}$=30 km/h, while the decrease is relatively weaker for $U_{p\infty}$=50 km/h at the same longitudinal position (X=0.5, 1). This latter confirms the trend observed in Figures 3, i.e., increasing airflow velocity induces a flow modification reinforcing the vortices which are supposed to transport the particles horizontally in addition to the vertical direction in the recirculation zone. Looking at Figure 4c, the longitudinal profile in the Y=–0.5 plane shows that the concentrations are more important farther behind the vehicle for X>2 than in the very near wake region. In this area, the concentrations are also higher at Y=–0.3 and –0.5 than at Y=0, this is especially more important than the air velocity is higher (Figure 4c–4d). Again, this observation underlines the importance of the vortices that could play a major role in the vehicle centerline in the vicinity of the vehicle, or farther behind the vehicle at the outer edges planes.

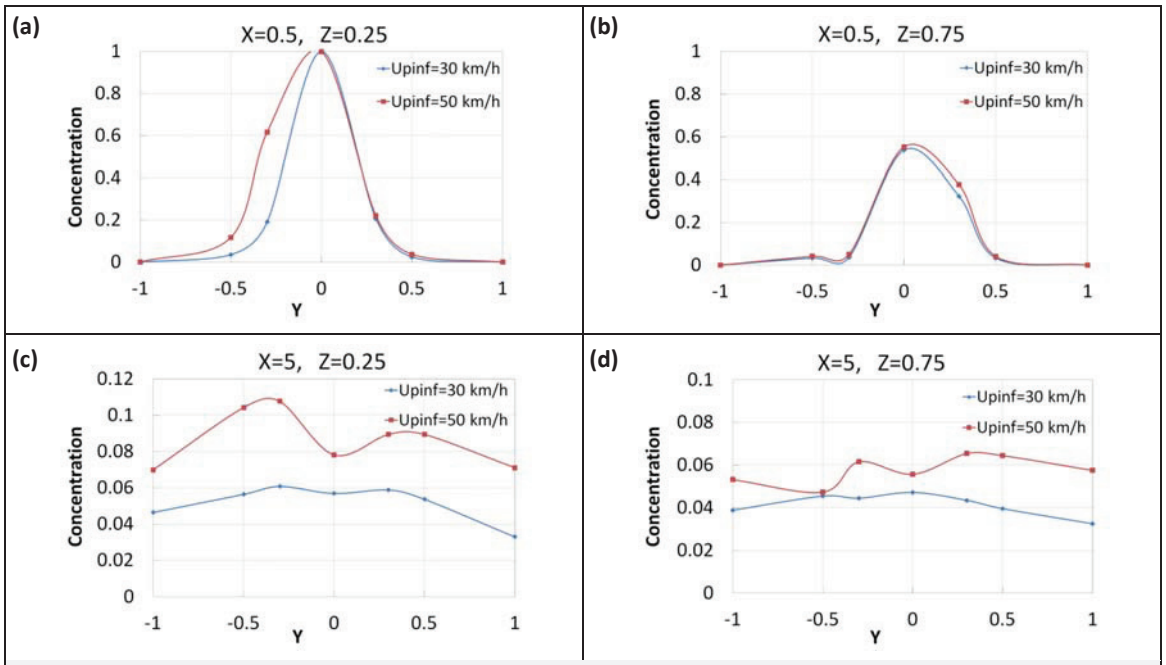

Figure 3. *Comparison of the horizontal profiles of dimensionless concentration at two different vehicle speeds, 30 km/h and 50 km/h, at X=0.5* ***(a)***, ***(b)*** *and X=5* ***(c)***, ***(d)***.

We also plot the time–averaged PNC results in terms of 2D contour plots at the *X*=5 vertical cross–section downstream of the vehicle. Considering Figure 5, scales are different. Each scale corresponds to the one obtained for the studied vehicle speed. Regardless of the changing in inflow velocity which induces a dilution, we aim to compare the local dispersion spreading. The effect of the vehicle speed on nanoparticles in the near wake region (for 2<*X*<5) is shown in the plane *Y*–Z at *X*=5 in Figure 5. The pair of longitudinal vortices is clearly highlighted by the nano-particles which play a role of passive tracer in this case. Our results also show that the dissymmetry of particle concentrations is still present. Nevertheless, we point out that it is shifted to the side of the emission point in a same manner as we found in the very near wake region. The concentration of nanoparticles which are trapped by the left longitudinal vortex is much more important than the right one. On the other hand, even at this distance from the vehicle, the diffusion is not Gaussian.

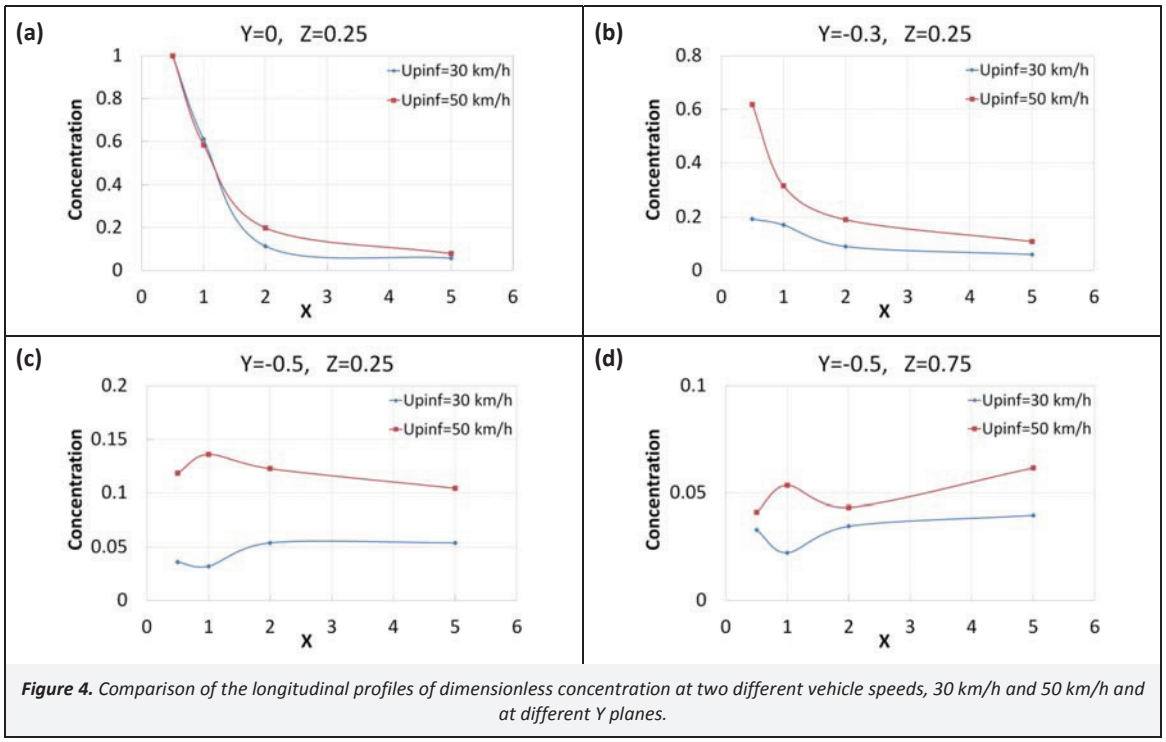

Figure 4. *Comparison of the longitudinal profiles of dimensionless concentration at two different vehicle speeds, 30 km/h and 50 km/h and at different Y planes.*

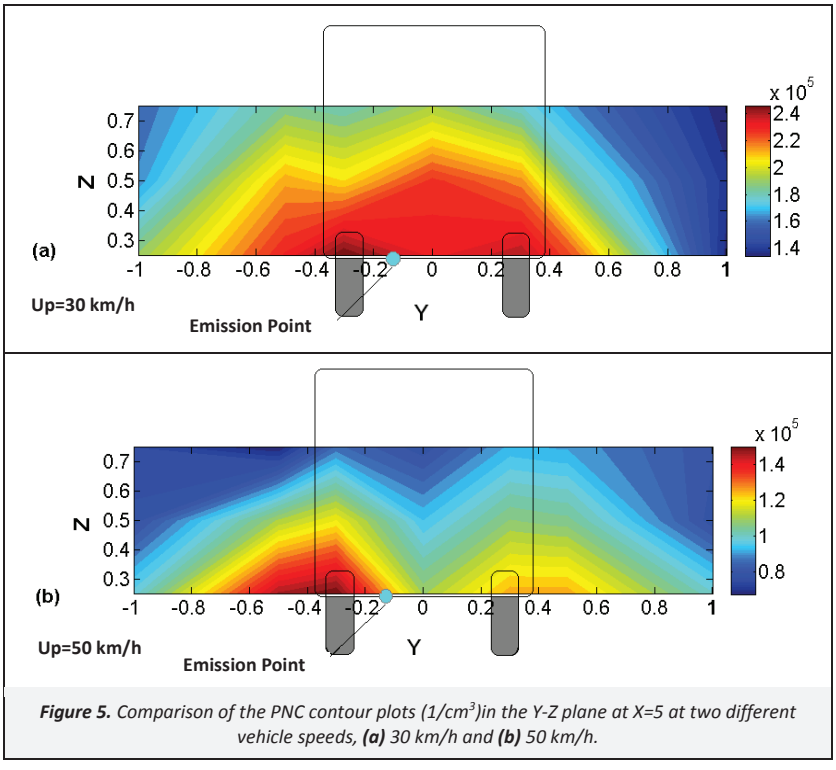

Figure 5. *Comparison of the PNC contour plots (1/cm^3)in the Y-Z plane at X=5 at two different vehicle speeds,* ***(a)*** *30 km/h and* ***(b)*** *50 km/h.*

All these experimental results allowed us to identify some typical behaviors. Depending on the vehicle speed, the emitted nanoparticles are supposed to be first trapped by vertical vortices developing in the recirculation region. At this stage they seem to be kept centered around Y=0 while their concentration is stretched in the vertical direction. This trend develops from X=0 to X=2. Downstream of this position, the pair of the longitudinal vortices coming from the outer edges becomes the predominant turbulent structures (Hucho, 1998) which results in the enhancement of the dispersion in the horizontal direction.

4. Conclusions

In the present study, we aimed at studying the dispersion of nanoparticles in the wake of a vehicle model. Different experiments were conducted in a wind tunnel for well–defined inflow conditions and scales according to some similitude laws. It is well–known that the near wake region is dominated by the coherent structures of different types and that nanoparticles are very sensitive to the interactions with turbulence, which in turn depends on the shape of the wake and on the flow dynamics. Based on these parameters, injecting and measuring ultrafine particle concentrations in the wake of a vehicle model in a wind tunnel lead us to a more comprehensive picture of the regions of UFP accumulation. We pointed out that the dynamic of the plume may be strongly affected by the vehicle speed. Furthermore, depending on the position of the exhaust pipe, which must be clearly defined, but also on the vehicle speed and on the distance from the rear of the vehicle, we showed that the recirculation region as well as the longitudinal vortices could play an important role. They are supposed to enhance the dispersion of the exhausted nanoparticles in both vertical and horizontal directions.

Nevertheless, the goal of this study was to demonstrate the feasibility of studying pollutant dispersion in wind–tunnel using real carbonaceous nanoparticles that could evolve in terms of size and concentration. This was successfully achieved. Indeed, the nanoparticles seem to accumulate in preferential zones and act as passive tracer that highlights the vortices which are generated in the vehicle near wake region. However, this study will be completed by characterizing the air flow at the same time to correlate these results with the mean and turbulent velocity fields developing downstream of the car. To achieve that goal, non–intrusive LDV measurements would be an asset. It is expected that such investigations would lead to an accurate description of the time and length scales characterizing the turbulent flow so the underline the importance of the vortices intensity and size in nanoparticles dispersion.

References

Carpentieri, M., Kumar, P., 2011. Ground–fixed and on–board measurements of nanoparticles in the wake of a moving vehicle. *Atmospheric Environment* 45, 5837–5852.

Carpentieri, M., Kumar, P., Robins, A., 2012. Wind tunnel measurements for dispersion modelling of vehicle wakes. *Atmospheric Environment* 62, 9–25.

Delfino, R.J., Sioutas, C., Malik, S., 2005. Potential role of ultrafine particles in associations between airborne particle mass and cardiovascular health. *Environmental Health Perspectives* 113, 934–946.

Diaz–Sanchez, D., Proietti, L., Polosa, R., 2003. Diesel fumes and the rising prevalence of atopy: An urban legend? *Current Allergy and Asthma Reports* 3, 146–152.

Evans, D.E., Harrison, R.M., Ayres, J.G., 2003. The generation and characterisation of elemental carbon aerosols for human challenge studies. *Journal of Aerosol Science* 34, 1023–1041.

Hucho, W.–H., 1998. *Aerodynamics of Road Vehicles: From Fluid Mechanics to Vehicle Engineering*, Butterworth–Heinemann, 566 pages.

Hudda, N., Eckel, S.R., Knibbs, L.D., Sioutas, C., Delfino, R.J., Fruin, S.A., 2012. Linking in–vehicle ultrafine particle exposures to on–road concentrations. *Atmospheric Environment* 59, 578–586.

Jeng, C.J., Kindzierski, W.B., Smith, D.W., 2007. Particle penetration through inclined and *L*–shaped cracks. *Journal of Environmental Engineering–ASCE* 133, 331–339.

Kanda, I., Uehara, K., Yamao, Y., Yoshikawa, Y., Morikawa, T., 2006. A wind–tunnel study on exhaust gas dispersion from road vehicles – Part I: Velocity and concentration fields behind single vehicles. *Journal of Wind Engineering and Industrial Aerodynamics* 94, 639–658.

Kittelson, D.B., Watts, W.F., Johnson, J.P., 2004. Nanoparticle emissions on Minnesota highways. *Atmospheric Environment* 38, 9–19.

Liu, D.L., Nazaroff, W.W., 2003. Particle penetration through building cracks. *Aerosol Science and Technology* 37, 565–573.

Mehel, A., Sagot, B., Taniere, A., Oesterle, B., 2012. On the mutual effect of the turbulent dispersion model and thermophoresis on nanoparticle deposition. *International Journal of Nonlinear Sciences and Numerical Simulation* 13, 417–425.

Mehel, A., Taniere, A., Oesterle, B., Fontaine, J.R., 2010. The influence of an anisotropic langevin dispersion model on the prediction of micro– and nanoparticle deposition in wall–bounded turbulent flows. *Journal of Aerosol Science* 41, 729–744.

Morawska, L., Ristovski, Z., Jayaratne, E.R., Keogh, D.U., Ling, X., 2008. Ambient nano and ultrafine particles from motor vehicle emissions: Characteristics, ambient processing and implications on human exposure. *Atmospheric Environment* 42, 8113–8138.

Oberdorster, G., Sharp, Z., Atudorei, V., Elder, A., Gelein, R., Kreyling, W., Cox, C., 2004. Translocation of inhaled ultrafine particles to the brain. *Inhalation Toxicology* 16, 437–445.

Pope, C.A., Burnett, R.T., Thun, M.J., Calle, E.E., Krewski, D., Ito, K., Thurston, G.D., 2002. Lung cancer, cardiopulmonary mortality, and long–term exposure to fine particulate air pollution. *JAMA–Journal of the American Medical Association* 287, 1132–1141.

Uhrner, U., von Lowis, S., Vehkamaki, H., Wehner, B., Brasel, S., Hermann, M., Stratmann, F., Kulmala, M., Wiedensohler, A., 2007. Dilution and aerosol dynamics within a diesel car exhaust plume – CFD simulations of on–road measurement conditions. *Atmospheric Environment* 41, 7440–7461.

Verrier, R.L., Mittleman, M.A., Stone, P.H., 2002. Air pollution – An insidious and pervasive component of cardiac risk. *Circulation* 106, 890–892.

Zhu, Y.F., Hinds, W.C., Krudysz, M., Kuhn, T., Froines, J., Sioutas, C., 2005. Penetration of freeway ultrafine particles into indoor environments. *Journal of Aerosol Science* 36, 303–322.

Zhu, Y., Hinds, W.C., Kim, S., Sioutas, C., 2002. Concentration and size distribution of ultrafine particles near a major highway. *Journal of the Air & Waste Management Association* 52, 1032–1042.